Biomechanical analysis of fatigue-related foot injury mechanisms in athletes and recruits during intensive marching

A. Gefen

Department of Biomedical Engineering, Faculty of Engineering, Tel Aviv University, Tel Aviv, Israel

Abstract—*An integrative analysis, comprising radiographic imaging of the foot, plantar pressure measurements, surface electromyography (EMG) and finite element (FE) modelling of the three-dimensional (3D) foot structure, was used to determine the effects of muscular fatigue induced by intensive athletic or military marching on the structural stability of the foot and on its internal stress state during the stance phase. The medial/lateral (M/L) tendency towards instability of the foot structure during marching in fatigue conditions was experimentally characterised by measuring the M/L deviations of the foot–ground centre of pressure (COP) and correlating these data with fatigue of specific lower-limb muscles, as demonstrated by the EMG spectra. The results demonstrated accelerated fatigue of the peroneus longus muscle in marching conditions (treadmill march of 2 km completed by four subjects at an approximately constant velocity of $8\,km\,h^{-1}$). Severe fatigue of the peroneus longus is apparently the dominant cause of lack of foot stability, which was manifested by abnormal lateral deviations of the COP during the stance phase. Under these conditions, ankle sprain injuries are likely to occur. The EMG analysis further revealed substantial fatigue of the pre-tibial and triceps surae muscles during intensive marching (averaged decreases of 36% and 40% in the median frequency of their EMG signal spectra, respectively). Incorporation of this information into the 3D FE model of the foot resulted in a substantial rise in the levels of calcaneal and metatarsal stress concentrations, by 50% and 36%, respectively. This may point to the mechanism by which stress fractures develop and provide the biomechanical tools for future clinical investigations.*

Keywords—*Muscle fatigue, Foot stability, Stress fractures, Foot–ground contact stress, Plantar pressure, Finite element model*

1 Introduction

NORMAL MUSCLE contraction during the stance phase of gait not only generates propulsion, but also maintains the stability of the foot during its interaction with the ground and protects its skeleton by absorbing some of the impacting stress waves (FYHRIE *et al.*, 1998; GEFEN *et al.*, 2001). During intensive and long marches, e.g. those carried out during military training, metabolic by-products reduce intra-muscular conduction velocity until a point where the muscles become unable to produce the desired forces (SVANTESSON *et al.*, 1998; GEFEN *et al.*, 2002). If such fatiguing activity does not cease at this stage, muscular control of the foot–shank joints deteriorates, and stability control and shock attenuation capacity are significantly reduced (GRIMSTON and ZERNICKE, 1993).

Under these conditions, the foot is vulnerable to injuries caused by two separate mechanisms. The first, an acute type of injury, can be caused by collapse of the subtalar joint (Fig. 1*a*) due to an impaired ability to resist dynamically the inversion/eversion tendency of the foot. The injury resulting from this loss of foot stability is generally termed as ankle sprain and can be accompanied by excessive strain or even microtears of the supportive ligaments.

The peroneal muscles play an important role in preventing this injury. Just before midstance begins, these muscles contract to prevent foot inversion and ensure safe completion of the roll-over process of stance. Indeed, fatigue-induced peroneal weakening and a delay of more than 60 ms in its contractile response were shown to be correlated with ankle sprains (STACOFF *et al.*, 1996). MILGROM *et al.* (1991) reported that the occurrence of ankle sprains is very common among military recruits during basic training, with a prevalence of around 18%.

The second type of injury can be induced by deterioration of the muscular ability to reduce effectively the level of impact of loads and the intensity of bone strains during the stance phase (GRIMSTON and ZERNICKE, 1993). Under normal conditions, muscular contraction decreases or eliminates local elevated
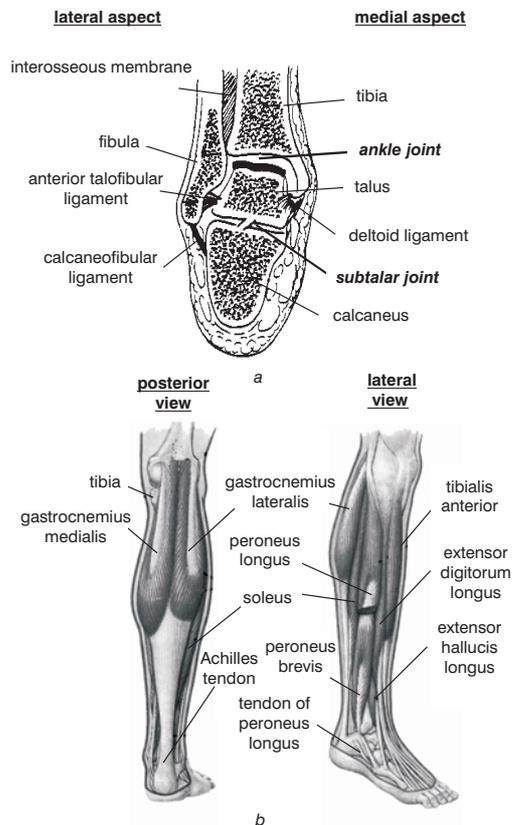
Fig. 1 *Anatomy of (a) foot–shank articulations and ligaments from posterior cross-sectional view (modified from* NORDIN *and* FRANKEL *(1989) and (b) muscles controlling foot–shank complex (modified from* THIBODEAU *and* PATTON *(1996))*

tensile stresses on the bone by producing counteracting compressive stresses; this function protects the cortical surface of the lower-limb skeleton, which provides more mechanical strength in compression than in tension (NORDIN and FRANKEL, 1989). The above protection mechanism is mainly achieved by contraction of the pre-tibial muscle group during heel-strike and by contraction of the gastro-soleus muscle group (Fig. 1b), also called the triceps surae, during push-off (DONAHUE and SHARKEY, 1999).

Weakened function of these muscle groups due to fatigue can lead to the generation of sites of locally intensified mechanical stresses within the lower-limb skeleton and, particularly, within the structure of the foot. These elevated stresses develop cyclically owing to the loading/unloading manoeuvres that take place during gait/marching. As long as the peak stresses and strains are kept within the physiological limit for bone, no damage appears (and the tissue may even be strengthened through functional adaptation). However, if physiological stress/strain limits are exceeded, local micro-failures at the cortical surface can be induced.

If the modelling and repair of bone in these regions is not sufficient, the generating micro-failures can accumulate into a stress (or overuse) fracture. In support of this contention, it was experimentally demonstrated that substantial formation of micro-cracks and creep damage occurred at sites of intensified stresses, when cortical bone specimens were cyclically loaded in simulated physiological conditions but without muscular protection (GRIMSTON and ZERNICKE, 1993).

Peak structural stresses that are generated within bones owing to inadequate muscular loading in fatigue conditions should therefore be considered as being useful parameters for the evaluation of potential risk of stress fractures. In a recent, large-scale epidemiological study among US Marine Corp recruits, the foot and ankle were found to be highly vulnerable

to stress fractures and suffered nearly 35% of the injuries (ALMEIDA *et al.*, 1999).

The generally accepted method for quantification of localised muscle fatigue, which also allows for experimental analysis of the above injury mechanisms, is to follow the shift in the spectral density of the electromyographic (EMG) signal towards lower frequencies, using the median frequency (MF) of the power spectrum as a guiding parameter (BASMAJIAN and DE LUCA, 1985). The shift towards the lower band was correlated with several physiological reactions of muscle tissue to fatigue, including reduction in the propagation velocity of signals along muscle fibres, alteration in the motor unit recruitment patterns and in the muscle activity level, as well as modification of the action potential and firing rate (MERLETTI and ROY, 1996).

Although the MF evolution during fatigue was shown to be affected by the length of the muscles (OKADA, 1987) and by the applied torques (GERDLE and KARLSSON, 1994), it is considered to be the best-recognised quantitative indicator of fatigue of skeletal muscles (XIAO and LEUNG, 1997). Experimental studies were recently conducted to correlate the decrease in the MF value and the actual force output during fatiguing activity of muscles (MANNION and DOLAN, 1996).

A fatigued system of lower-limb muscles is also much less efficient at controlling the stability of the foot structure (STACOFF *et al.*, 1996). An effective way to evaluate the tendency of the foot to inversion/eversion motion during the stance phase and thereby to assess its structural stability in fatigue conditions is to measure abnormal deviations in the trajectory of the centre of pressure (COP). Increased activity of the foot evertors (e.g. the peroneus longus) moves the COP medially and the body's centre of mass laterally to maintain foot stability, and, consequently, body balance. Similarly, increased invertor (e.g. tibialis anterior or extensor hallucis longus) activity moves the COP laterally and the body's centre of mass medially (HAN *et al.*, 1999).

It should be emphasised that invertor/evertor muscles can also act as plantar flexors and dorsiflexors, so that there is an interdependency of anterior/posterior (A/P) and medial/lateral (M/L) movement of the COP. Because of the relatively small width of the foot, a fine active control of its M/L stability is required (BAUBY and KUO, 2000). WINTER (1995) showed that any moments generated by the invertors/evertors that are greater than 10 Nm would cause the foot to roll over its medial or lateral aspects.

In the present study, surface EMG and foot–ground pressure (FGP) measurements were integrated with a computational model of the three-dimensional (3D) foot structure (GEFEN *et al.*, 2000), to analyse the effects of muscular fatigue, induced by athletic or military marching, on the structural stability of the foot and the structural stresses developing within its skeleton. Thus the potential roles of marching-related lower-limb muscular fatigue in the occurrence of ankle sprains and in the development of stress fractures of the foot could be discussed.

2 Methods

2.1 *Integrative experimental–computational approach*

This study employed an integrative experimental and computational analysis for a comprehensive study of the biomechanics of the foot during the stance phase of athletic or military marching. Knowledge of the dynamic stress distribution within and between the structural components of the foot is essential to the understanding of their respective functions during different gait/marching conditions. Realistic modelling of the foot's structure during the stance phase of gait necessarily relies on meaningful experimental characterisations of its

kinematics and dynamics, including the foot's skeletal motion, the foot–ground contact pressure and the electrical activity of the controlling muscles. To acquire these essential data, a system of experimental and computational biomechanical tools was developed and is described in detail elsewhere (GEFEN et al., 2000). For completeness, a brief review follows:

(i) Skeletal positions and bone orientations at each of the characteristic sub-phases of stance (e.g. heel-strike, midstance, push-off) were measured using a digital radiographic fluoroscopy (DRF) system*. Plantar pressures were acquired using the optical contact pressure display (CPD) method (Fig. 2), which was developed by Arcan and his colleagues to enable a simultaneous, fast imaging process of a large contact area by employing a sensitive birefringent integrated optical sandwich (see BROSH and ARCAN (1994) for a review of the CPD method). Construction of a DRF/CPD gait platform that integrated the CPD method into a DRF system allowed simultaneous acquisition of foot skeletal motion and foot–ground plantar pressures during the stance phase (GEFEN et al., 2000; 2001; 2002).

(ii) A set of dimensionless dynamic stress intensity parameters (DSIPs) were determined, based on the dynamic foot–ground pressure pattern that was generated during the stance phase. These DSIPs were used for experimental evaluation and characterisation of the foot structure (e.g. the sharpness of

the calcaneus, the rise of the arch etc.). A statistical database for characterising DSIP values in normal subjects was developed from the accumulated information.

(iii) The electrical activity of specific muscles controlling foot position was evaluated by means of surface electrodes and a six-channel portable system of EMG amplifiers. Simultaneous CPD measurements of plantar pressure enabled demonstration of the effects of an alteration in the muscular activity pattern (i.e. weakness of certain muscles due to fatigue) on the foot–ground contact pressure.

A 3D computational model of the foot's structure during the stance phase, which incorporated realistic geometric and material properties of both the skeletal and soft tissue components, was developed according to the above experimental data. This model included 17 bony elements, representing the entire foot skeleton, 38 ligaments, the plantar fascia, a fat pad at the sole of the foot and 11 different muscles that controlled the foot's motion. The foot's position during the stance phase, the forces of the controlling muscles and the ankle joint load were fed into the simulation.

Using a finite element solver, the distribution of contact stresses between the foot model and simulated ground, as well as the stress distribution within the foot's structure, was obtained. Hence, regions of elevated structural stresses for characteristic positions of stance (e.g. heel-strike, midstance and push-off) were located. Validation of the model predictions of structural stress distribution was achieved by comparison of simulated and measured DSIP characteristics of the foot–ground pressure pattern, according to predefined statistical t-tests (GEFEN et al., 2000).

In this study, the above integrative experimental–computational system of biomechanical tools was first applied to analyse the structural stability of the foot in conditions of lower-limb muscular fatigue induced by intensive marching. The M/L tendency of instability of the foot's structure during marching in fatigue conditions was experimentally characterised using the DSIP approach. The M/L deviations of the foot–ground COP during marching were experimentally correlated with fatigue of specific lower-limb muscles, as demonstrated by the EMG spectra. The computational 3D foot model was then applied to explore alterations in the structural stress distributions due to the marching-induced muscular fatigue patterns, to identify risk factors for fatigue-related injuries and devise means for obviating them.
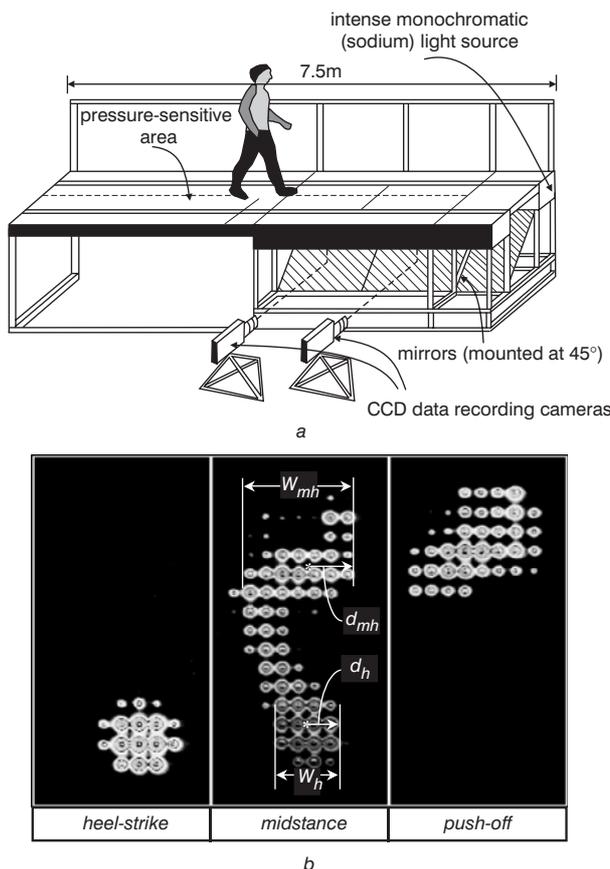

Fig. 2 *Contact pressure display (CPD) method: (a) setup of 7.5 m long gait platform and cameras in the Musculoskeletal Biomechanics Laboratory of Tel-Aviv University; (b) typical high-resolution CPD images of foot–ground pressure during heel-strike, midstance (with parameters defining eccentricities of centre of pressure under heel and metatarsal heads) and push-off*

2.2 *Muscular fatigue experimental model*

A group of six easily identifiable muscles controlling the foot–shank joints was selected for the present analysis. Analysis of fatigue of these muscles was carried out using surface EMG electrodes that allow for non-invasive measurement of muscle activity with minimum interference with the natural musculoskeletal kinematic/dynamic behaviour. To obtain reliable data from the surface EMG electrodes while avoiding 'cross-talk' between muscle layers, only superficial muscles were selected, as shown in Fig. 1b and Table 1.

These muscles are among the most significant contributors to the production of the levering forces and moments that act on the structure of the foot. The gastro-soleus group, for instance, produces over 90% of the pulling forces used to lift the heel during push-off (CAILLIET, 1983; GLITSCH and BAUMAN, 1997), whereas the tibialis anterior, extensor hallucis longus and peroneus longus also play a role in stabilising the foot's structure and the ankle joint throughout the stance phase (RODGERS, 1995). The tibialis posterior, although an important invertor of the subtalar joint, was not monitored for EMG activity, because its deep location in the

Table 1 *Muscles controlling foot–shank articulation complex*

Muscle	Primary function	Origin	Insertion
gastrocnemius lateralis	plantar flexion	lateral femoral condyle	calcaneus through Achilles tendon
gastrocnemius medialis	plantar flexion	medial femoral condyle	calcaneus through Achilles tendon
soleus	plantar flexion	tibia and head of fibula (underneath gastrocnemius)	calcaneus through Achilles tendon
tibialis anterior	foot inversion; dorsiflexion	lateral condyle and proximal shaft of tibia	first cuneiform and base of first metatarsal
extensor hallucis longus	dorsiflexion	midportion of shaft of fibula	distal phalanx of big toe
peroneus longus	foot eversion; plantar flexion	fibular head and proximal shaft	distal phalanx of big toe

shank which limits reliable surface EMG measurements (PEROTTO and DELAGI, 1996).

Two male (25 and 17 years old) and two female (28 and 17 years old) athletes volunteered to participate in this study and follow the protocol summarised in Table 2, to demonstrate the effects of muscular fatigue during intensive marching on the stability and function of the foot. Marching exercises were carried out on a mechanical treadmill, thus allowing continuous EMG monitoring of the fatigue process.

In each march, the athletes were required to complete a course of 2 km at a nearly constant velocity of $8 \, \mathrm{km \, h^{-1}}$ (transient velocity deviations of $\pm 25\%$ were allowed). These marching conditions are typical in military training and some sportive marching conditions (BROSH and ARCAN, 1994).

Before and immediately following each exercise, the evolution of the plantar pressures during the stance phase of gait was measured during marches (post-exercise measurements were carried out with a delay of no longer than 1 min after completion of the 2 km course). Plantar pressures were measured using the 7.5 m long CPD gait platform at Tel Aviv University (TAU), which contains 52 optical sensors per area of $10 \times 10 \, \mathrm{cm^2}$ (Fig. 2a).

The plantar pressure evolutions during marching at approximately $8 \, \mathrm{km \, h^{-1}}$ on the CPD gait platform were acquired for all subjects at 30 frames $\mathrm{s^{-1}}$ (30 Hz), while subjects were barefooted and while they were wearing their own shoes (three trials were repeated for each case). The eccentricities of the COP under two specific regions of interest, the heel and metatarsal heads, were derived from the CPD images of the FGP's evolution acquired during the stance phase of gait to obtain the M/L tendency towards instability of the foot during stance, both before and following exercise. The DSIP dimensionless representations of the eccentricities of the COP under the heel e_h and metatarsal heads e_{mh} are defined as follows (GEFEN et al., 2000; 2002):

$$e_h = \frac{1}{2} - \frac{d_h}{w_h} \tag{1}$$

$$e_{mh} = \frac{1}{2} - \frac{d_{mh}}{w_{mh}} \tag{2}$$

where w_h and w_{mh} are the transverse widths of the maximally loaded contact areas under the heel and metatarsal heads, respectively, and d_h and d_{mh} are the transverse distances of the COP from the medial boundaries of the contact areas under the heel and metatarsal heads, respectively (Fig. 2b). Hence, positive values for e_h and e_{mh} indicate medial eccentricities, and negative values indicate lateral eccentricities. The COP's parameters of eccentricity were used to evaluate M/L shifts of the COP of the foot–ground and shoe–ground pressure patterns that could be related to muscular fatigue.

The EMG activities of the six lower-limb muscles of interest (Table 1) were acquired simultaneously with the CPD contact-pressure images (Fig. 2b). Electromyographic activities of these muscles were also acquired continuously throughout each treadmill march. Continuous monitoring and recording of EMG activity during treadmill marches were preferred over a different measurement approach that had been tested in a preliminary stage of the experiments, in which EMG measurements were carried out before and after completion of outdoor marches in field conditions. This decision was taken as since post-exercise body recovery and consequent underestimation of the actual fatigue conditions could not be avoided in the outdoors preliminary experiments, while the subject was prepared for the EMG/CPD measurements upon completion of the march.

A mechanical treadmill[†] was used for inducing muscular fatigue due to marching. The treadmill was equipped with handrails, a belt with a walking area of $1.26 \times 0.36 \, \mathrm{m}$ and digital displays of distance and speed. The use of a treadmill offered a great advantage as the subjects did not need to be followed around with the EMG measuring equipment (impractical in the case of long-distance walking), and the speed and slope could be easily controlled. It should be noted that differences can exist between treadmill and over-ground locomotion, e.g. in a longer push-off sub-phase during treadmill walking (SAVELBERG et al., 1998). These differences are mainly associated with psychological factors, such as the changed optical flow and lack of adaptation to treadmill locomotion. In the present study, a mechanical treadmill powered by the fore-aft ground reaction force was preferred over a treadmill equipped with an electrical motor, to eliminate

Table 2 *Experimental protocol of treadmill marching test (CPD = contact pressure display)*

Stage of experiment	Subject's activity	Measurement
Pre-exercise	30 inversion/eversion motions of foot	EMG
	march (with and without shoes) on CPD platform	EMG/CPD
March exercise	march of 2 km at $8 \, \mathrm{km \, h^{-1}}$ on treadmill	EMG
Post-exercise	march (with and without shoes) on CPD platform	EMG/CPD
	30 inversion/eversion motions of foot	EMG

[†]Fliptrak Co., Taiwan

any possible electronic interference with the EMG measurement system.

We calibrated the speed display of the treadmill prior to each test by measuring the time taken for the 2.74 m long belt to complete ten revolutions over ten different speeds. The actual treadmill speeds and the speeds displayed on its monitor were found to be highly correlated (with a correlation coefficient $r = 0.99$). Based on the standard error of estimation, we could be 95% confident that the digitally displayed speed, which was maintained at around 8 km h^{-1}, did not differ from the actual belt speed by more than 0.1 km h^{-1}.

Considering the importance of adequate peroneal activity to foot stability, as described in Section 1, EMG signals produced by the peroneus longus were also acquired during 30 inversion/eversion motions of the foot that were carried out before and after completion of the treadmill marching exercises (Table 2).

The EMG data were simultaneously acquired from the six muscles of interest (Table 1) using a six-channel portable system of EMG amplifiers[‡] connected in parallel. After the skin had been shaved and scrubbed with alcohol, disposable Ag/AgCl surface electrode discs[**] with a diameter of 9 mm were attached to the subject's skin at locations recommended by PEROTTO and DELAGI (1996) for monitoring the particular muscles (Table 1) while avoiding cross-talk. For each muscle, two electrodes were placed at a distance of approximately 30 mm in the direction of the muscle fibres. A reference electrode, shared by the six measurement channels, was placed on the bony part of the lateral aspect of the knee joint. Cables and interfaces were shielded to eliminate interferences.

Signals were pre-amplified by factors in the range of 2000–5000 (depending on the subject) and captured by a 12-bit A/D board[††] at a sampling rate of 1 kHz. The evolution of the power spectrum function of each of the six muscles of interest was calculated off-line by means of a signal-processing software package. The duration of EMG signal bursts and the evolution of the MF during the marching test were calculated for each of the six muscles of interest at time intervals of 1 min, according to the following algorithm:

Constant timeframe windows for the fast Fourier transform (FFT) analysis were set for each muscle at 80% of the duration of the muscle signal burst measured in the last minute of exercise, to allow a consistent evaluation of the decrease in MF throughout the march. To evaluate the activity timeframes of the EMG bursts consistently, signal envelopes were calculated (Fig. 3) using a digital band, fourth-order Butterworth 7–11 Hz filter (GLITSCH and BAUMAN, 1997; DE LUCA, 1984; ROSEN et al., 1999). Initiation of the burst was recognised when the burst envelope exceeded 5% its maximum value, and termination was recognised when the burst envelope value dropped beneath 5% of the maximum.

The timeframe from initiation to termination was determined as the burst length, and the centre point of the burst was calculated as being the average time point between initiation and termination events. The timeframe window of interest for FFT analysis was taken as being bounded between -40% and $+40\%$ of the burst length, as measured from the centre point of the burst. For each muscle, a Hanning window was then used to modify these timeframe windows containing 80% of the durations of signal bursts, before the FFT analysis was applied to obtain the burst's spectra. The power spectrum functions that were calculated using the FFT analysis were smoothed with a 'moving average' filter of 21 points and normalised with respect to the maximum value achieved during exercise. The
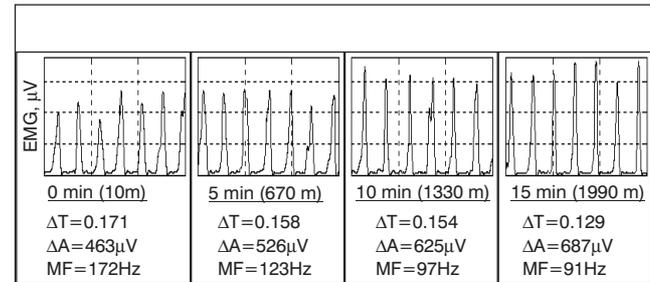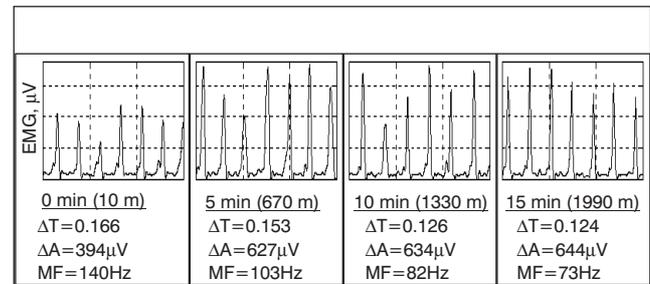
Fig. 3 Evolution of surface EMG signal envelope and characteristic parameters, at time intervals of 5 min, for (a) peroneus longus and (b) gastrocnemius lateralis muscles, during treadmill marching at velocity of 8 km h^{-1}. ΔT = signal burst duration, ΔA = signal burst amplitude, MF = median frequency. Values are averaged for ten gait cycles

evolution of the MF of each muscle was then derived from its set of power spectra in terms of percentage decrease from the initial value.

2.3 Computational modelling of marching in muscular fatigue conditions

The 3D computational model of the foot (GEFEN et al., 2000) was employed to study the biomechanical effects of lower-limb muscular fatigue induced by intensive marching on the internal stresses developing within the foot structure. It was decided to concentrate upon the heel-strike and push-off sub-phases of gait, as the foot–ground loads transferred at these stages are maximum (NORDIN and FRANKEL, 1989). Finite element analysis was predetermined to result in the structural stress distribution in terms of von Mises equivalent stresses ($\sigma_{v.M.}$), which weighs the effect of all principal stresses (σ_1, σ_2, σ_3) according to the relationship

$$\sigma_{v.M.} = \left\{ \frac{1}{2}[(\sigma_1 - \sigma_2)^2 + (\sigma_2 - \sigma_3)^2 + (\sigma_3 - \sigma_1)^2] \right\}^{\frac{1}{2}} \quad (3)$$

Analysis of stress distributions along important cross-sections of the foot further provides a detailed characterisation of its loading state during the stance phase and allows for comparative studies of different gait conditions. Five planar cross-sections through the 3D model's geometry (marked S$_1$ to S$_5$) were selected for this purpose (Fig. 4).

The locations of the planar cross-sections were chosen so that each of them crosses one of the five rays of the foot (e.g. the 1st section crosses the 1st metatarsal and the 1st phalange). All of the planes are vertical; each plane passes through the centre of its respective metatarsal head and through the calcaneal base. Planes S$_1$ and S$_5$ pass through the two end points of a virtual line (of approximately 2 cm in length) that crosses the calcaneus–ground contact surface at its widest area; planes S$_2$, S$_3$ and
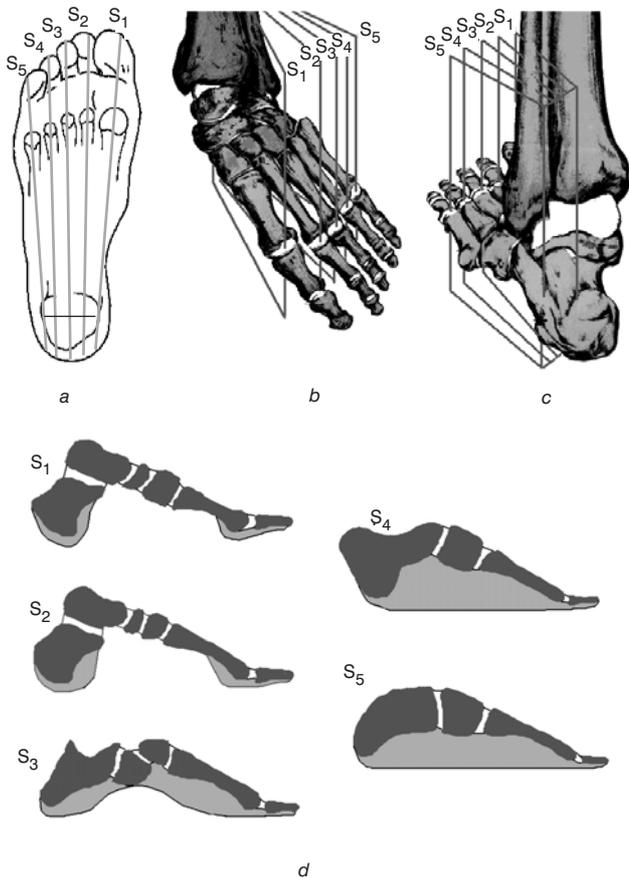
Fig. 4 *Five selected planar sections (marked as S_1–S_5) presented from (a) plantar view, (b) anterior view and (c) posterior view; (d) cross-sectional geometry of 3D foot model at five selected planar sections S_1–S_5*

S_4 cross this line at equal intervals (Fig. 4a). The 2D geometry of each cross-section is shown in Fig. 4d. Thus the complete set of these five cross-sections yields a convenient representation of the arched structure of the foot and allows for further comparative analysis of the stresses developing within its skeleton in the normal and muscular fatigue conditions.

In the absence of any literature reports characterising the relationship between the foot musculature's force output during fatigue and its MF decline, and in view of the infeasibility of measuring these relationships for individual muscles, it was assumed for computational simulation purposes that, during fatigue, the foot musculature exerts forces in proportion to its maximum force output, which, according to MANNION and DOLLAN (1996), is linearly correlated with the decrease in the MF. Therefore 'treadmill marching'-induced muscular fatigue was simulated using the 3D foot model by the normal force output of individual muscle groups, given in GEFEN *et al.* (2000),

being reduced proportionally to the decrease observed in their MF when the marching exercise was completed.

According to the observed evolution of the MF of each of the six muscles of interest during the marching tests (and as further reported in Section 3), stresses evidenced by the model were solved under two conditions

(*a*) simulated moderate fatigue, defined as 80% of the normal force output given in GEFEN *et al.* (2000), and severe fatigue, defined as 60% of the normal force output of the pre-tibial muscles (tibialis anterior and extensor hallucis longus) during heel-strike.

(*b*) simulated moderate fatigue, defined as 80% of the normal force output, and severe fatigue, defined as 60% of the normal force output of the triceps surae muscles (soleus, gastrocnemius lateralis and gastrocnemius medialis) during push-off.

The resultant stress concentrations predicted by the model were identified, and the dependency of their values upon the reduction in force output of these specific muscle groups was quantified.

3 Results

3.1 Experimental results

The reduction in the duration of the EMG signal bursts and in the MF values of the burst spectra, resulting from intensive 2 km treadmill marches, were calculated for the six selected lower-limb muscles according to the protocol described in Section 2, and the scores are given in Table 3.

The most prominent decreases in duration of the EMG signal bursts due to fatigue were found to occur in the peroneus longus and gastrocnemius lateralis muscles. Moreover, substantial reductions of 15–20% in the duration epochs of the signal bursts due to fatigue were also observed in the gastrocnemius medialis and soleus muscles (Table 3). The evolution of the surface EMG signal envelopes and the changes in the duration of the signal bursts, signal amplitudes and MF values of the peroneus longus and gastrocnemius lateralis muscles during a representative treadmill march are presented in Fig. 3.

The average duration of the signal bursts of the peroneus longus was shown to decrease by more than 20% (i.e. nearly to its minimum value), after 10 min of treadmill marching, when about two-thirds of the marching distance was completed. The EMG/CPD simultaneous measurements that had been carried out before and immediately following the treadmill marches (Table 2) further showed that this decrease in the signal burst duration is the outcome of a negligible amount of peroneal activity from midstance to push-off.

The MF values in the power spectra of all six selected muscles decreased considerably (in a range of 25–50%) during fatigue (Table 3), whereas the maximum MF decrease was recorded for the peroneus longus and gastrocnemius lateralis muscles. Fatigue was evident in these muscles after no more than

Table 3 *Summary of average changes (in percentages of unstressed values) in epoch duration of EMG signal bursts and MFs of six lower-limb muscles as result of 2 km laboratory treadmill marching tasks. Data acquired during 10 gait cycles in first minute of march are used as initial values and compared with data acquired during 10 gait cycles in last minute of march*

Muscle	Change in epoch duration of EMG signal burst, % of initial burst epoch values	Change in median frequency, % of initial MF values
Gastrocnemius lateralis	79 ± 5	56 ± 5
Gastrocnemius medialis	91 ± 5	68 ± 5
Soleus	86 ± 3	58 ± 5
Tibialis anterior	95 ± 2	61 ± 5
Extensor hallucis longus	96 ± 2	67 ± 5
Peroneus longus	77 ± 4	56 ± 6

10 min (approximately 1300 m) of treadmill marching, when reductions to less than 63% of the initial MF values were recorded for both of them (Fig. 3). When the peroneus longus was tested by inversion/eversion tasks (Table 2), the shift in the MF towards the lower band was more pronounced than during gait, exceeding 50%.

Single-subject-designed statistics were used to test the significance of the substantial drops in the MF of the peroneus longus, pre-tibial and triceps surae muscles during the marching exercises. Significance was set at the 5% level. For this statistical analysis, marching tasks were divided into three stages of equal duration (of around 5 min each, depending upon the subject).

The averaged MF values recorded through each stage (averaging about five data points for each muscle) were compared, showing a statistically significant drop in the MF of all the above-listed muscles (Table 1) for all the subjects tested ($p < 0.01$). This drop was statistically significant ($p < 0.01$), both from the first stage of the march to its mid-part, and from the mid-part to its final part. This shows that all the muscles of interest were considerably affected by the 2 km marching exercises, which were therefore well suited for studying the consequent effects on the stability and internal stresses of the foot under fatigue.

The COP eccentricities under the heel (e_h) and metatarsal heads (e_{mh}) were calculated using equations (1) and (2) from CPD data of gait tests performed with the EMG/CPD setup, before and immediately following the treadmill marches. The COP eccentricity evolutions during gait that had been carried out pre- and post-exercise are presented in Fig. 5. Muscular fatigue was shown to alter the COP trajectory significantly. The heel's eccentricity e_h (measurable until midstance terminates and the heel rises toward push-off) is shown to be more laterally shifted post-exercise compared with its pre-exercise orientation, whereas the peak lateral shift appears during midstance (Fig. 5). The metatarsal head's eccentricity e_{mh}, (measurable from midstance to the end of stance) is similarly shifted laterally in fatigue, whereas the peak shift occurs between midstance and push-off.
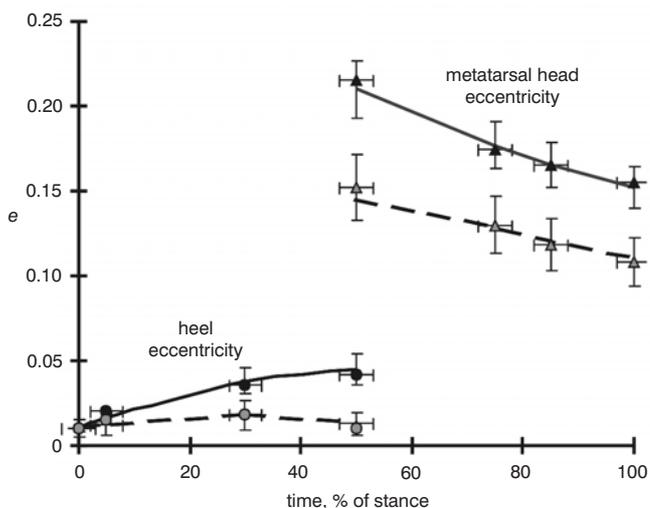
3.2 Computational results

The experimental analysis of the EMG data obtained during marches from the small group of athletes resulted in an averaged reduction of 36% in the MF of the pre-tibial (tibialis anterior and extensor hallucis longus) muscle group signals and of 40% in the MF of the triceps surae (gastrocnemius lateralis, gastrocnemius medialis and soleus) muscle group signals (Table 3). Subsequently, and in accord with the computational protocol described in Section 2, stresses in the foot model were solved under two conditions:

(i) simulated moderate fatigue (80% of normal force output) and severe fatigue (60% of normal force output) of the pre-tibial muscles during heel-strike.

(ii) simulated moderate fatigue (80% of normal force output) and severe fatigue (60% of normal force output) of the triceps surae muscles during push-off.

The resulting von Mises stress distributions on the 3D model and along the characteristic cross-sections, S_1 and S_2 are given in Fig. 6. Peak stresses were shown to rise significantly with muscle fatigue in both cases. A reduction of 40% in the pre-tibial force output during heel-strike in simulated severe muscular fatigue
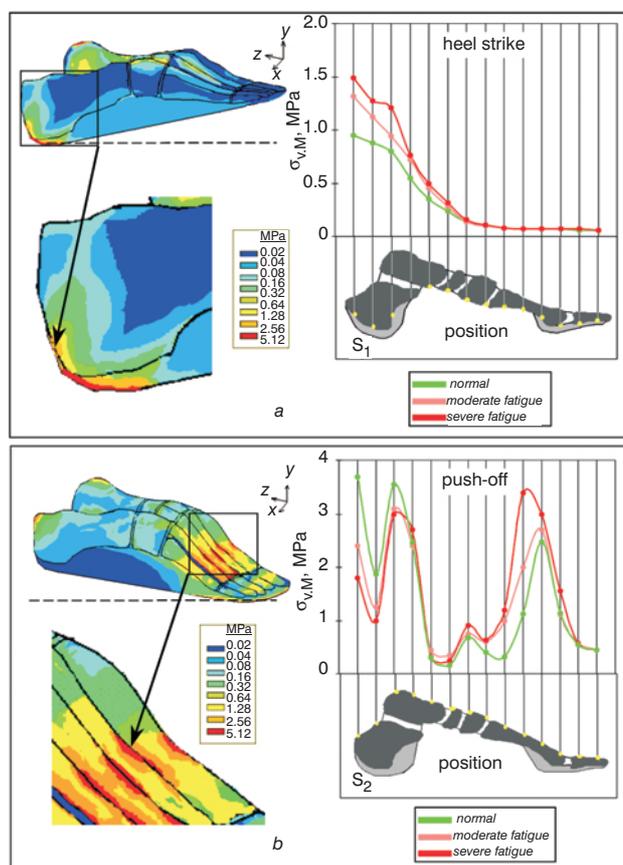

Fig. 6 *Effects of muscle fatigue on formation of elevated stresses leading to stress fractures: (a) (left) simulated von Mises calcaneal stress distribution during heel-strike in moderate pre-tibial muscle fatigue conditions, and (right) von Mises stress distribution along plantar aspect of 1st ray of foot in normal, moderate and severe fatigue conditions; (b) (left) simulated von Mises 2nd metatarsal stress distribution during push-off in moderate triceps surae muscle fatigue conditions, and (right) von Mises stress distribution along dorsal aspect of 2nd ray of foot in normal, moderate and severe fatigue conditions. Moderate and severe fatigues were defined as activation of 80% and 60% of muscle force, respectively*

Fig. 5 *Representative evolution of average eccentricities of centre of pressure under (○ ●) heel, e_h, and (△ ▲) metatarsal heads, e_{mh}, during stance phase of barefooted gait (—) before and (- - -) immediately following treadmill marches of 25-year-old athlete (bars denote measurement ranges). Smaller values for e_h and e_{mh} indicate more laterally shifted eccentricity of COP*

conditions caused peak calcaneal stresses to rise by 50%. Similarly, a reduction of 40% in the triceps surae force output during push-off in simulated severe muscular fatigue conditions caused peak second metatarsal stresses to rise by 36%.

4 Discussion

An integrative experimental-computational methodology was developed in this study to relate the fatigue of specific muscles during intensive marching to the foot's tendency towards M/L instability and to the stress distribution developing within its skeleton. The findings provide better understanding of the mechanisms of common fatigue-related injuries of the foot: ankle sprains and stress fractures.

The dramatic reductions in activity and force output manifested by the decrease in the MF of the peroneus longus and gastrocnemius lateralis muscles from midstance to push-off provide a reasonable explanation for the lateral shift of the COP eccentricities during fatigue, as reported in Section 3. The fatigued gastrocnemius lateralis cannot effectively counteract the gastrocnemius medialis to produce an efficient, vertically orientated resultant levering force on the hindfoot towards push-off. Instead, the deviation of the resultant force that is exerted on the hindfoot by these muscles results in an inverting moment on the foot's structure. As the fatigued peroneus longus no longer produces sufficient contractile forces to restrain the tendency for subtalar inversion at this time, the COP is shifted laterally, indicating a deterioration in foot stability, as demonstrated in Fig. 5. Therefore the results of the EMG/CPD analysis suggest that the foot may be most vulnerable to ankle sprains from midstance to the end of the push-off sub-phase during intensive marching.

In view of the mechanism of fatigue-related ankle sprain injuries suggested above, the characteristics unique to sports/military marching should be emphasised. Athletes and military recruits are generally required not to reduce their marching velocity in fatigue conditions. Thus, although their muscular control in this state has deteriorated, the impacting ground-reaction forces (GRFs) generated during their locomotion are still considerably high (military recruits may also be required to carry heavy loads that further increase the GRFs). The elevated moments caused by the intensified GRFs increase the likelihood of subtalar joint collapse and ankle sprain. Other muscles and body segments (e.g. the hip abductors and the trunk) can also be affected by the development of fatigue and further deteriorate the control of the foot's stability; it is quite possible that, in fatigue, the hip musculature is unable to control the position of the head–arms–trunk segments as precisely as it does in the unfatigued state. In many cases, athletes/recruits are subjected, not only to muscle fatigue, but also to aerobic exhaustion, which may further deteriorate their neuromuscular control performances, e.g. the capability required to recover balance when subtalar joint collapse is initiated. Hence, the vulnerability of athletes/recruits to ankle sprains is likely to increase with muscular fatigue.

Several factors other than muscular fatigue may further contribute to ankle sprains, e.g. changes in the material properties of the ligaments that restrain the foot-shank joints that occur as a result of an injury. As more than one factor may be involved in ankles that have been repetitively sprained, it is important to develop analysis tools that can accommodate multiple risk factors. The present approach and, especially, the use of a realistic computational model not only provide convincing evidence for the identification of the factors acting to produce the damage, but also allow examination of these factors, both dependently and independently of one another, to determine the relative contribution of each to the risk of injury.

Peak stresses in the foot skeleton were shown to rise significantly with muscle fatigue during heel-strike as well as during push-off. In both cases, the rise in the peak stress values could be associated with the increase in the bending moments that are applied to the calcaneus during heel-strike and to the metatarsals during push-off. It is generally accepted that contraction of the plantar flexor muscles helps to counteract the moments placed on the metatarsals by the elevated dynamic skeletal loads during the push-off stage (RODGERS, 1995). It seems that muscular fatigue reduces the rate and force of contraction of the triceps surae, thereby increasing metatarsal stress. Similarly, weakened pre-tibial muscle contractions during heel-strike increase the bending moments applied to the calcaneus by the impacting ground reaction force (GRF) acting on its distal plantar aspect and by the body load acting on its proximal dorsal aspect. The above mechanisms could therefore be significant contributors to the development of stress fractures in these bones.

With the 3D computational model, it is possible quantitatively to characterise stresses in the foot's skeleton during the entire stance phase of gait: simulated severe muscle fatigue significantly increased both calcaneal and metatarsal stresses, particularly at the posterior aspect of the calcaneus and second metatarsal, where the von Mises stresses increased by 50% and 36%, respectively. This can be correlated with clinical findings indicating that stress fractures of the foot most commonly occur in the calcaneus and metatarsal bones (GRIMSTON and ZERNICKE, 1993).

As the living bone is visco-elastic and the simulations were performed by a quasi-static analysis, which assumed that bones are linearly elastic, there may have been some overestimation of the magnitudes of the resulted stresses. Nevertheless, this approach is highly useful for evaluation of the relative effects of muscle fatigue on skeletal loading and for isolating the role of fatigue among other conditions that affect the tendency to stress fractures, such as alteration in nutritional factors or hormonal perturbations (GRIMSTON and ZERNICKE, 1993).

Considering the above findings, sports and military authorities may recommend physical training directed towards enhancing the strength and endurance of muscles that are specifically related to the 'marching' pattern of fatigue, to improve foot stability and impact attenuation abilities during prolonged fast marching or running. By applying the presently developed integrative set of biomechanical tools to conduct large-scale clinical research on subjects with similar body and age characteristics, accurate and statistically significant identification of the muscles that are most closely implicated in fatigue-related skeletal injuries during marching could be obtained. Accordingly, sports and military training protocols could be regulated, in light of the effects of muscular fatigue, and thereby the prevalence of fatigue-related injuries could be reduced. Further development of this approach can also contribute to the evaluation of risk factors for different populations, e.g. military recruits with low/high arch structure, to assess their vulnerability to fatigue-related injuries and to consider protective means when indicated, e.g. shock absorbing footwear or ankle braces.

References

ALMEIDA, S. A., WILLIAMS, K. M., SHAFFER, R. A., and BRODINE, S. K. (1999): 'Epidemiological patterns of musculoskeletal injuries and physical training', *Med. Sci. Sports Exerc.*, **31**, pp. 1176–1182

BASMAJIAN, J. V., and DE LUCA, C. J. (1985): 'Muscles alive' (Williams and Wilkins, Baltimore, 1985), pp. 125–127

BAUBY, C. E., and KUO, A. D. (2000): 'Active control of lateral balance in human walking', *J. Biomech.*, **33**, pp. 1433–1440

BROSH, T., and ARCAN, M. (1994): 'Toward early detection of the tendency to stress fractures', *Clin. Biomech.*, **9**, pp. 111–116

CAILLIET, R. (1983): 'Foot and ankle pain' (F.A. Davis Company, Philadelphia, 1983)

DE LUCA, C. J. (1984): 'Myoelectric manifestations of localized muscle fatigue in humans', *Crit. Rev. Biomed. Eng.*, **11**, pp. 251–265

DONAHUE, S. W., and SHARKEY, N. A. (1999): 'Strains in the metatarsals during the stance phase of gait: implications for stress fractures', *J. Bone Joint Surg.*, **81**, pp. 1236–1243

FYHRIE, D. P., MILGROM, C., HOSHAW, S. J., SIMKIN, A., DAR, S., DRUMB, D., and BURR, D. B. (1998): 'Effect of fatiguing exercise on longitudinal bone strain as related to stress fracture in humans', *Ann. Biomed. Eng.*, **26**, pp. 660–665

GEFEN, A., MEGIDO-RAVID, M., ITZCHAK, Y., and ARCAN, M. (2000): 'Biomechanical analysis of the three-dimensional foot structure during gait – a basic tool for clinical applications', *J. Biomech. Eng.*, **122**, pp. 630–639

GEFEN, A., MEGIDO-RAVID, M., and ITZCHAK, Y. (2001): 'In vivo biomechanical behavior of the human heel pad during the stance phase of gait', *J. Biomech.*, **34**, pp. 1661–1665

GEFEN, A., MEGIDO-RAVID, M., ITZCHAK, Y., and ARCAN, M. (2002): 'Analysis of muscular fatigue and foot stability during high-heeled gait', *Gait & Posture*, **15**, pp. 56–63

GERDLE, B., and KARLSSON, S. (1994): 'The mean frequency of the EMG of the knee extensors is torque dependent both in the unfatigued and the fatigued states', *Clin. Physiol.*, **14**, pp. 419–432

GLITSCH, U., and BAUMAN, W. (1997): 'The three-dimensional determination of internal loads in the lower extremity', *J. Biomech.*, **30**, pp. 1123–1131

GRIMSTON, S. K., and ZERNICKE, R. F. (1993): 'Exercise-related stress response in bone', *J. Appl. Biomech.*, **9**, pp. 2–14

HAN, T. R., PAIK, N. J., and IM, M. S. (1999): 'Quantification of the path of center of pressure (COP) using an F-scan in-shoe transducer', *Gait & Posture*, **10**, pp. 248–254

MANNION, A. F., and DOLAN, P. (1996): 'Relationship between myoelectric and mechanical manifestations of fatigue in the quadriceps femoris muscle group', *Eur. J. Appl. Physiol.*, **74**, pp. 411–419

MERLETTI, R., and ROY, S. (1996): 'Myoelectric and mechanical manifestations of muscle fatigue in voluntary contractions', *J. Orthop. Sports Phys. Ther.*, **24**, pp. 342–353

MILGROM, C., SHLAMKOVITCH, N., FINESTONE, A., ELDAD, A., LAOR, A., DANON, Y. L., LAVIE, O., WOSK, J., and SIMKIN, A. (1991): 'Risk factors for lateral ankle sprain: a prospective study among military recruits', *Foot Ankle*, **12**, pp. 26–30

NORDIN, M., and FRANKEL, V. H. (1989): 'Basic biomechanics of the musculoskeletal system' (Lea & Febiger, Philadelphia, PA, 1989)

OKADA, M. (1987): 'Effect of muscle length on surface EMG wave forms in isometric contractions', *Eur. J. Appl. Physiol.*, **56**, pp. 482–486

PEROTTO, A., and DELAGI, E. F. (1996): 'Anatomic guide for the electromyographer – the limbs and trunk' (Charles C. Thomas, Springfield, IL, 1996)

RODGERS, M. M. (1995): 'Dynamic foot biomechanics', *J. Orthop. Sports Phys. Therapy*, **21**, pp. 306–315

ROSEN, J., FUCHS, M. B., and ARCAN, M. (1999): 'Performances of Hill-type and neural network muscle models – toward a myosignal-based exoskeleton', *Comput. Biomed. Res.*, **32**, pp. 415–439

SAVELBERG, H. C. M., VORSTENBOSCH, A. T. M., KAMMAN, E. H., VAN DE WEIJER, J. G. W., and SCHAMBARDT, H. C. (1998): 'Intra-stride belt-speed variation affects treadmill locomotion', *Gait & Posture*, **7**, pp. 26–34

STACOFF, A., STEGER, S., STUSSI, E., and REINSCHMIDT, C. (1996): 'Lateral stability in the sideward cutting movements', *Med. Sci. Sports Exerc.*, **28**, pp. 350–358

SVANTESSON, U., OSTERBERG, U., THOMEÉ, R., and GRIMBY, G. (1998): 'Muscle fatigue in a standing heel-rise test', *Scand. J. Rehabil. Med.*, **30**, pp. 67–72

THIBODEAU, G. A., and PATTON, K. T. (1996): 'Anatomy and physiology' (Mosby, St. Louis)

XIAO, S., and LEUNG, S. C. (1997): 'Muscle fatigue monitoring using wavelet decomposition of surface EMG', *Biomed. Sci. Instrum.*, **34**, pp. 147–152

WINTER, D. A. (1995): 'Human balance and posture control during standing and walking', *Gait & Posture*, **3**, pp. 193–214

Author's biography

Dr AMIT GEFEN is a Lecturer in the Department of Biomedical Engineering at the Faculty of Engineering of Tel Aviv University, Israel. He received his BSc in Mechanical Engineering, in 1994, and his MSc, in 1997, and PhD, in 2001, in Biomedical Engineering, from Tel Aviv University. His experience is in foot and gait biomechanics, as well as in bone biomechanics and in the application of computational modelling methods to the design and biomechanical optimisation of implants.